Available online at www.sciencedirect.com
SCIENCE DIRECT
Thin Solid Films 475 (2005) 291–297
thin solid films
www.elsevier.com/locate/tsf

Electrochemical behavior of diamond-like carbon films for biomedical applications

Ho-Gun Kim[a], Seung-Ho Ahn[a], Jung-Gu Kim[a,*], Se Jun Park[b], Kwang-Ryol Lee[b]

[a]Department of Advanced Materials Engineering, Sungkyunkwan University, 300 Chunchun-Dong, Jangan-Gu, Suwon 440-746, South Korea
[b]Future Technology Research Division, Korea Institute of Science and Technology, P.O. Box 131, Cheongryang, Sungbuk-Gu, Seoul 130-650, South Korea

Available online 11 September 2004

Abstract

Diamond-like carbon (DLC) films have several advantages in biomedical applications such as high hardness, chemical inertness, low friction and electrical insulation. Furthermore, DLC-coated STS 316L films have been reported to have a good biocompatibility. In addition, corrosion resistance is the first consideration for the biomaterials to be used in the body. DLC films have been deposited onto substrates of STS 316L using rf plasma-assisted chemical vapor deposition (PACVD) with benzene (C_6H_6) or a mixture of C_6H_6 and silane (SiH_4) as process gas. Three kinds of DLC films were prepared as a function of bias voltage and Si incorporation. Corrosion behavior of DLC films was investigated by electrochemical techniques (potentiodynamic polarization test and electrochemical impedance spectroscopy (EIS)) and surface analytical techniques (atomic force microscopy (AFM) and scanning electron microscopy (SEM)). The electrolyte used in this test was a 0.89% NaCl of pH 7.4 at temperature of 37 °C. Electrochemical measurements showed that DLC films with higher bias voltage and Si incorporation could improve corrosion resistance in the simulated body fluid environment.
© 2004 Elsevier B.V. All rights reserved.

Keywords: DLC; Porosity; Protective efficiency; SEM; EIS

1. Introduction

The materials selected for use in an orthopaedic implant were developed after years of research into the chemical and physical properties of different host materials. Ideally, the material of choice will not only be biocompatible but also have corrosion-resistant properties that match the biomaterial being replaced human bone. Stainless steel substrate as orthopaedic implants is mainly used to improve biocompatibility [1]. However, the body fluid is very corrosive, which can lead not only to uniform corrosion but also to crevice attack and pitting for metal alloys. Corrosion of orthopaedic implants is critical because it can adversely affect biocompatibility. Corrosion is the first consideration of implants of any type that is to be used in the body because metal ion release takes place mainly due to corrosion of orthopaedic implants [2]. Moreover, wear debris produced from movement of joints can lead to wear-corrosion causing degradation of corrosion resistance [3]. DLC films for biomedical applications were a great interest to researchers in recent years [4–6] because of their excellent properties such as electric insulation, low friction, high wear resistance, high hardness, corrosion resistance and biocompatibility [7–10]. The superior mechanical performance and corrosion resistance make DLC films the preferred candidate for protective films. Many authors have noted the potential of DLC films as a coating for orthopaedic implants. However, it is difficult to obtain films that exhibit good adhesion to steel substrates [11]. Other authors have informed on the use of amorphous silicon intermediate layers to improve the adhesion of DLC films deposited using rf plasma-assisted chemical vapor deposition (PACVD) method [12,13].

This study is focused on the evaluation of the electrochemical behavior of amorphous hydrogenated carbon (a-C:H) films prepared by rf PACVD as a function of bias voltage and Si incorporation.

* Corresponding author. Tel.: +82 31 290 7360; fax: +82 31 290 7371.
E-mail address: kimjg@skku.ac.kr (J.-G. Kim).

0040-6090/$ - see front matter © 2004 Elsevier B.V. All rights reserved.
doi:10.1016/j.tsf.2004.07.052

2. Experimental

2.1. Materials preparation

Si-wafer and stainless steel (STS 316L) were used as substrate materials. Stainless steel substrate of 37 mm diameter was cut from a 2-mm-thick sheet. Sample surfaces were mechanically polished down to an average roughness of R_a~0.3 μm using SiC papers and diamond paste.

The DLC films were prepared by capacitively coupled rf PACVD. Schematic diagram of the rf PACVD method for DLC deposition is given in Fig. 1. A substrate was placed on the water-cooled cathode where 13.56 MHz rf power was delivered through the impedance-matching network. Before deposition, substrates were precleaned using argon ion for 15 min at bias voltage of −400 V and pressure 9.975×10^{-3} Torr. Precursor gases used were benzene (C_6H_6) for a-C:H films and a mixture of C_6H_6 and silane (SiH_4) for Si-DLC films. The vacuum vessel was pumped by a roots and backing pump to a base pressure of approximately 2.0×10^{-5} Torr prior to deposition. A dense Si interlayer of thickness approximately 0.01 μm was deposited onto the steel substrate prior to DLC films. The interlayer was deposited primarily to control and set-up a residual stress gradient between the DLC film and the steel substrate. A coating thickness of about 1 μm was achieved in all cases. The film thickness was analyzed by alpha-step profilometer.

2.2. Corrosion testing

2.2.1. Electrochemical measurements

A 0.89% NaCl solution was made from reagent grade NaCl with distilled water and was thoroughly deaerated by bubbling high-purity nitrogen with a flow rate of 25 cc/min.

Potentiodynamic polarization tests and electrochemical impedance spectroscopy (EIS) measurements were carried out in a 0.89% NaCl solution of pH 7.4 at temperature of 37 °C. This solution was simulated as a human body environment. The exposed coating area was 1 cm^2. Reference and counter electrodes were used for a saturated calomel and a pure graphite, respectively. Potentiodynamic polarization tests were preformed using an EG & G PAR 273A for DC measurement. Prior to the potentiodynamic polarization tests, the specimens were kept in the solution for 6 h in order to establish the open circuit potential (OCP). The potential of the electrode was swept at a rate of 0.166 mV/s from the initial potential of −250 mV versus E_{corr} to the final potential of 1500 mV.

EIS tests were obtained using a Zahner IM6e system using commercial software (THALES) program for AC measurement. A perturbation AC potential of amplitude 10 mV (peak-to-peak) was applied over a frequency range between 10 kHz and 10 mHz. The impedance diagrams were interpreted based on the equivalent circuit using THALES fitting program.

In addition, the extent of delamination area (A_d) and volume fraction of water uptake (V) were determined from the experimental values of pore resistance (R_{pore}) and coating capacitance (C_{coat}) obtained by the impedance diagrams on the basis of the equivalent circuit [14].

$$A_d = R^o_{pore}/R_{pore} \quad (1)$$

$$R^o_{pore} = \rho d\left(\Omega - cm^2\right) \quad (2)$$

$$V = \log[C_{coat}(t)/C_{coat}(0)]/\log 80 \quad (3)$$

where R^o_{pore} was characteristic value for the corrosion reaction at the metal–coating interface, d coating thickness, ρ the coating resistivity, $C_{coat}(t)$ the coating capacitance at a

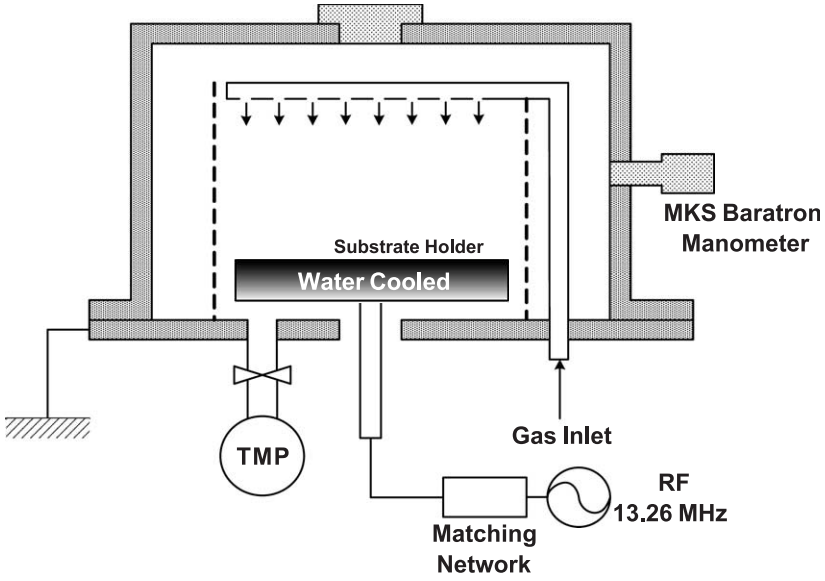

Fig. 1. Schematic diagram of the PACVD method for DLC deposition.

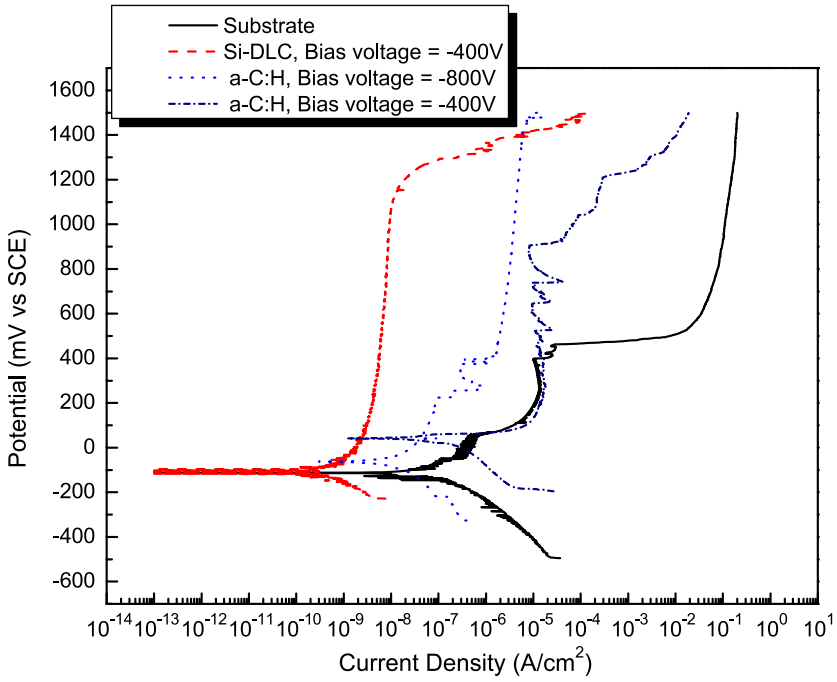

Fig. 2. Potentiodynamic polarization curves in deaerated 0. 89% NaCl solution at 37 °C (pH=7.4).

given time (t) and $C_{coat}(0)$ the coating capacitance at the initial time.

2.2.2. Porosity and protective efficiency

Porous coatings do not inhibit the diffusion of aggressive agents through the coating. Owing to the generation of corrosion resulting from the contact between the substrate and the corrosive environment, the porosity measurement in the coating is essential to determine the corrosion-resistant coating. In addition, porosity can provide an easy fracture path for adhesion failure. By using electrochemical techniques, it is possible to estimate the porosity of DLC films. The porosity can be determined from the measured polarization resistance. Matthes et al. [15] established an empirical equation to estimate the porosity (P) of the films.

$$P = \frac{R_{pm(substrate)}}{R_{p(coating-substrate)}} \times 10^{-|\Delta E_{corr}/\beta_a|} \quad (4)$$

where P was the total coating porosity, R_{pm} the polarization resistance of the substrate and R_p the measured polarization resistance of the coated steel system. ΔE_{corr} is the difference of the corrosion potential between the coating and the substrate and β_a is the anodic Tafel slope of the substrate. In addition, protective efficiency (P_i) of the coating was determined from the polarization curve by Eq. (5):

$$P_i = 100\left(1 - \frac{i_{corr}}{i^o_{corr}}\right) \quad (5)$$

where i_{corr} and i^o_{corr} indicate that the corrosion current densities in the presence and absence of the coating, respectively [16].

2.3. Surface analysis

Surface roughness of coating was measured using atomic force microscopy (AFM) operated in the contact mode. Scanning electron microscopy (SEM) was also used to examine the surface morphology of coatings as well as the corroded surfaces of tested specimens.

3. Results and discussion

3.1. Corrosion properties

In order to investigate the protection abilities and stabilities against localized corrosion of coatings, potentio-

Table 1
Results of potentiodynamic polarization tests

Specimen	E_{corr} (mV)	i_{corr} (nA/cm^2)	β_a (V/decade)	β_c (V/decade)	R_p ($\times 10^3$ Ω−cm^2)	Protective efficiency (%)	Porosity
Substrate	−114.6	249.3	0.1285	0.1868	132.7	–	–
Si-DLC, bias voltage=−400 V	−111.6	0.06486	0.3527	0.06077	347492.9	99.97	0.00037
a-C:H, bias voltage=−800 V	−63.11	15.33	0.4868	0.1839	3785.5	93.85	0.01393
a-C:H, bias voltage=−400 V	40.55	103	0.5402	0.1293	440.3	58.68	0.01869

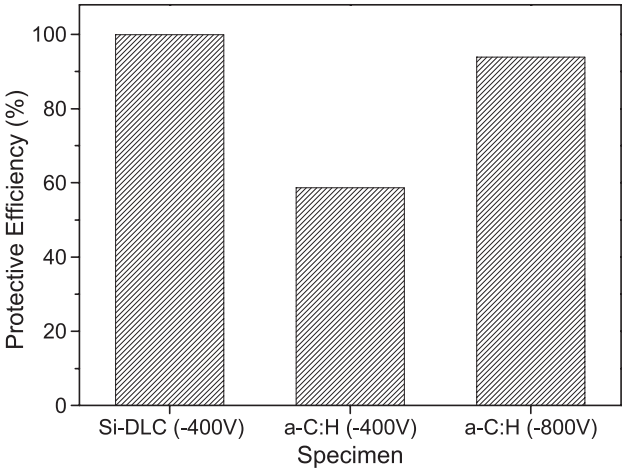

Fig. 3. Comparison of protective efficiency for the coatings.

dynamic polarization measurements were performed. Potentiodynamic polarization curves for DLC films are shown in Fig. 2 and electrochemical parameters are presented in Table 1. The measured corrosion potential (E_{corr}), corrosion current density (i_{corr}), porosity (P) and protective efficiency (P_i) are given in the table. It can be seen that the passive film was formed on the specimen. Especially, Si-DLC film was well passivated, with low passive current density and wide passive potential range. DLC films with Si incorporation and higher bias voltage clearly prevent pitting entirely in the passive potential range and promote repassivation. The corrosion current density with Si incorporation and higher bias voltage in the same film is much lower than that of a-C:H (bias voltage of −400 V). A combination of the equation of Matthes et al. [15] and the electrochemical determinations gives a porosity of 0.01869 for a-C:H (bias voltage = −400 V), 0.01393 for a-C:H (bias voltage = −800 V) and 0.00037 for Si-DLC (bias voltage = −400 V).

Fig. 3 shows the protective efficiency calculated from corrosion current density described in Table 1. As shown in Fig. 3, the protective abilities of coatings increased with the higher bias voltage and with Si incorporation in coatings. The highest protective efficiency was 99.97% of Si-DLC

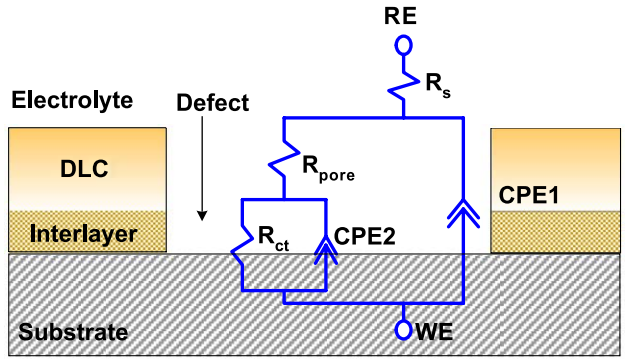

Fig. 4. Equivalent circuit for the DLC film system (WE, working electrode; RE, reference electrode).

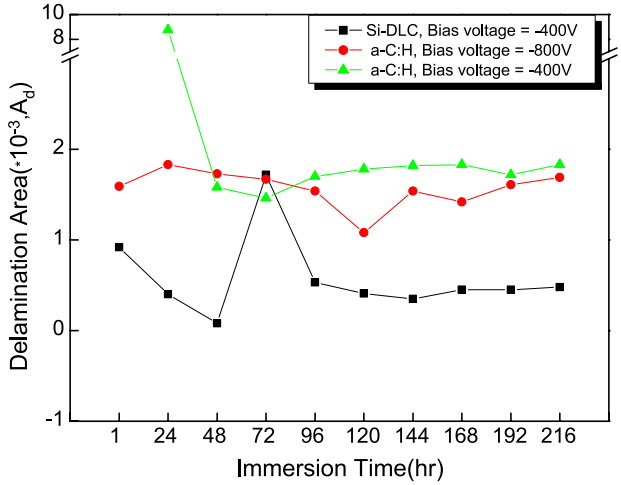

Fig. 5. Delamination area as a function of immersion time.

film. These results are consistent with porosity values. The lower the calculated porosity, the higher is the protective efficiency. This is closely related to the corrosion protective ability and durability of coatings under conditions of applications.

An electrode interface undergoing an electrochemical reaction can often be modelled by an equivalent circuit, as shown in Fig. 4. The equivalent circuit consists of the following elements; R_s corresponds to the solution resistance of the test electrolyte between the working electrode and the reference electrode and C_{coat} is the capacitance of the coating including pores in the outer layer coating. R_{pore} is the pore resistance resulting from the formation of ionic conduction paths across the coating. C_{dl} is the double-layer capacitance of the coating within the pit and R_{ct} is the charge transfer resistance of the coating/substrate interface. The deviation of the impedance from pure capacitance behavior can be attributed to inhomogeneity in the coating system and nonuniform diffusion. There is some deviation of the data at several low-frequency points. This can be attributed to the behavior of constant phase element (CPE).

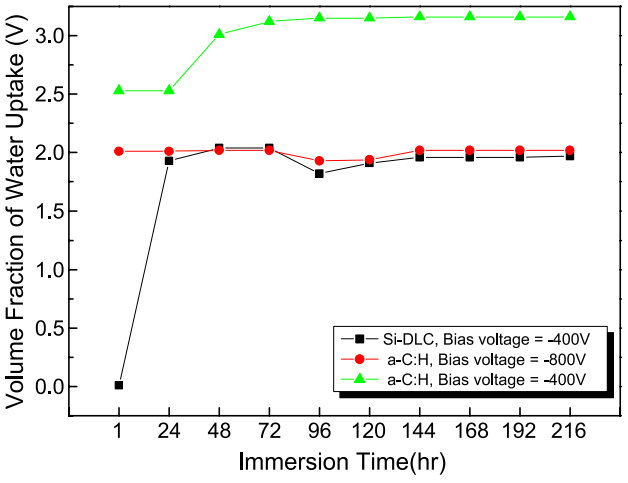

Fig. 6. Volume fraction of water uptake as a function of immersion time.

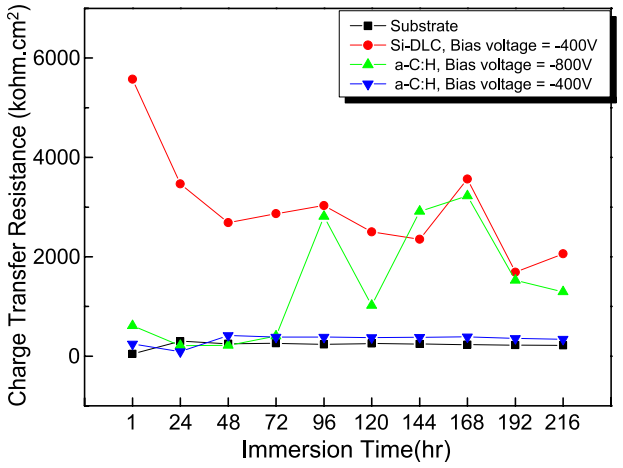

Fig. 7. Charge transfer resistance values as a function of immersion time.

It can also be described in terms of a distribution of relaxation times [17]:

$$Z_{\mathrm{CPE}} = Z_{\mathrm{o}}(j\omega)^{-n}$$

where Z_{o} is the adjustable parameter used in the nonlinear least squares fitting, ω is angular frequency and the factor n, defined as a CPE power, is an adjustable parameter that always lies between 0.5 and 1.

The results obtained from EIS tests were usually used to monitor the change of delamination area (A_{d}) and volume fraction of water uptake (V). Figs. 5–7 show the delamination area (A_{d}), the volume fraction of water uptake (V) and the charge transfer resistance (R_{ct}) values of specimens, respectively. After an initial decrease of delamination area during the 48-h immersion, Si-DLC film shows a constant variation, as shown in Fig. 5. Moreover, delamination area was affected by the volume fraction of water uptake through porous coating. Delamination area and volume fraction of water uptake with Si incorporation and higher bias voltage are much lower than those of a-C:H (bias voltage = −400 V), as shown in Figs. 5 and 6. The lower delamination area and volume fraction of water uptake with Si incorporation and higher bias voltage mean less amount of absorbed water compared to a-C:H (bias voltage = −400 V).

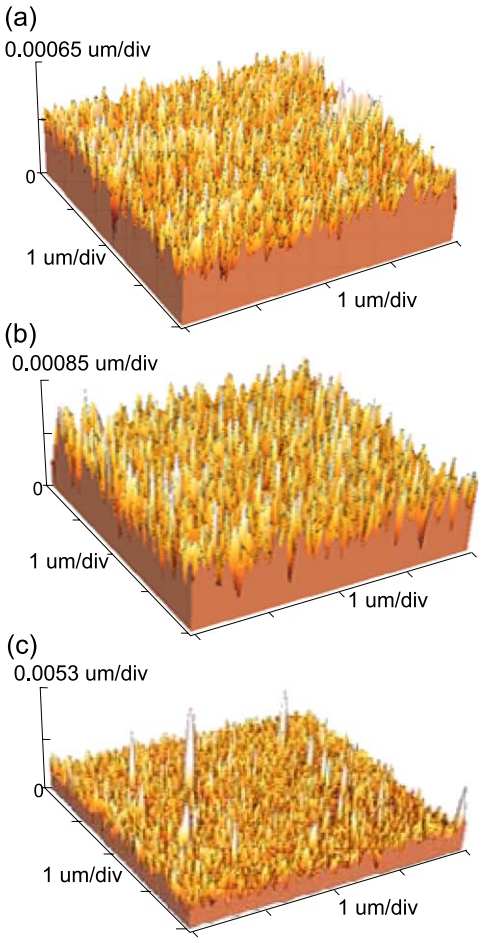

Fig. 8. AFM images showing uniformity of DLC coatings deposited at bias voltage and Si incorporation: (a) Si-DLC, bias voltage=−400 V; (b) a-C:H, bias voltage=−800 V; (c) a-C:H, bias voltage=−400 V.

Table 2
Result of electrochemical impedance spectroscopy measurements

Exposure time		R_{s} (Ω−cm^2)	CPE1		R_{pore} ($\times 10^3$ Ωcm^2)	CPE2		R_{ct} ($\times 10^3$ Ω−cm^2)	A_{d} ($\times 10^{-3}$)	V
			C_{coat} ($\times 10^{-9}$ F/cm^2)	n (0–1)		C_{dl} ($\times 10^{-9}$ F/cm^2)	n (0–1)			
120 h	Substrate	32.96	46440	1	78.9	175200	1	252.2	–	–
	Si-DLC (−400 V)	700.7	20.8	0.9921	3.43	47.47	0.7483	2501	0.41	1.91
	a-C:H (−800 V)	11.39	5.2	0.8675	81.8	508.5	0.914	1018	1.08	1.94
	a-C:H (−400 V)	929.1	878.4	0.6016	92.4	714.2	1	372.5	1.70	3.15
168 h	Substrate	34.57	47980	1	76.53	169400	1	230.2	–	–
	Si-DLC (−400 V)	882.4	26.4	1	3.175	43	0.7375	3566	0.45	1.96
	a-C:H (−800 V)	3.235	7.64	0.892	62.42	815.4	0.9328	3226	1.42	2.02
	a-C:H (−400 V)	719.8	892.4	0.6017	89.99	120.6	1	387.8	1.83	3.16
216 h	Substrate	33.29	48210	1	73.4	174200	1	218.2	–	–
	Si-DLC (−400 V)	4.308	27.1	0.9602	2.9	47.05	0.5329	2062	0.48	1.97
	a-C:H (−800 V)	18.2	7.74	0.8884	52.5	749.4	0.8843	1292	1.69	2.02
	a-C:H (−400 V)	696	899.4	0.6099	89.9	542.2	1	342	1.83	3.16

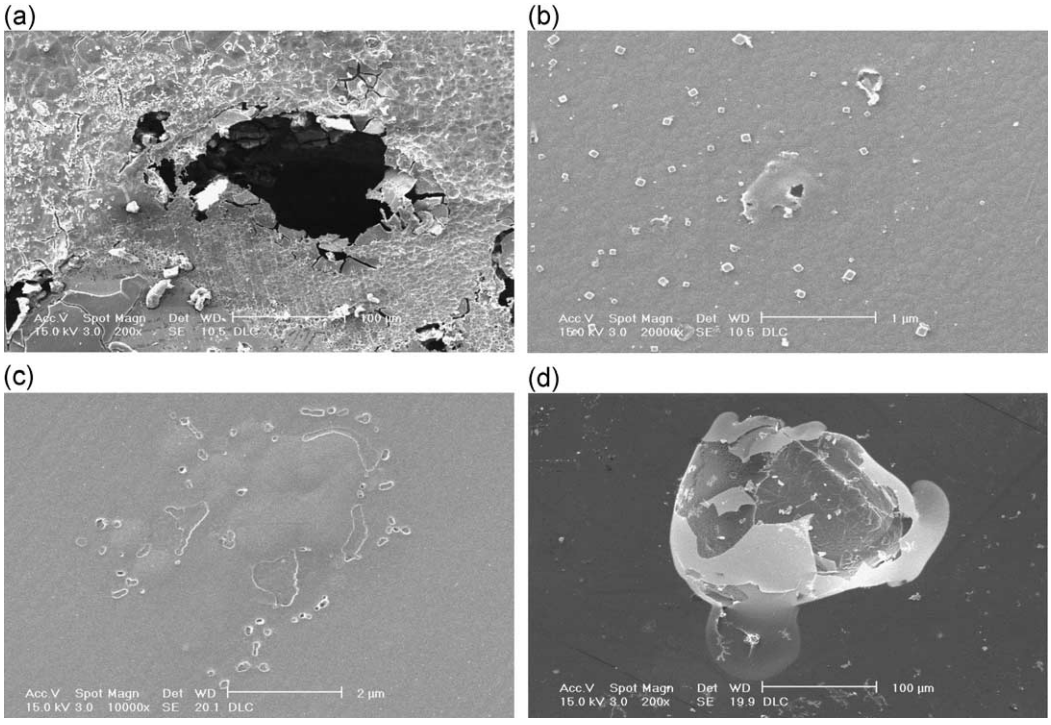

Fig. 9. SEM images showing surface morphologies of DLC coatings deposited at bias voltage and Si incorporation: (a) substrate; (b) Si-DLC, bias voltage=−400 V; (c) a-C:H, bias voltage=−800 V; (d) a-C:H, bias voltage=−400 V.

The excellent agreement between the delamination area and the volume fraction of water uptake over the test period suggests that porosity is strongly related to the coating delamination and the fraction of the substrate which is wetted by the electrolyte through defects. According to Table 2, the charge transfer resistance is relatively decreased with increasing the immersion time. The charge transfer resistance (R_{ct}) values with Si incorporation and higher bias voltage are much higher than that of a-C:H (bias voltage = −400 V), as presented in Fig. 7. It is important that a high R_{ct} value indicates good corrosion resistance. Consequently, it was shown that corrosion resistance of DLC films with Si incorporation and higher bias voltage would be improved in corrosive environment.

3.2. Surface analysis

Fig. 8 shows the coating surface roughness of the specimens with deposited condition. The coating surface roughness of 0.0906 μm for Si-DLC film, 0.2326 μm for a-C:H (bias voltage = −800 V) and 0.6157 μm for a-C:H (bias voltage = −400 V) was examined through the AFM measurements. This shows that DLC films with Si incorporation and higher bias voltage have improved coating surface roughness. Fig. 9 shows the surface morphologies of the specimens after potentiodynamic polarization test. This clearly indicates that DLC films with Si incorporation and higher bias voltage have excellent pitting and corrosion resistance, and no significant damage has been observed.

4. Conclusions

(1) DLC films with Si incorporation and higher bias voltage showed lower corrosion current density and porosity than a-C:H (bias voltage = −400 V), indicating better corrosion resistance.
(2) An increase of bias voltage and Si incorporation reduced delamination area (A_d) and volume fraction of water uptake (V) in DLC films. In addition, charge transfer resistance (R_{ct}) values with Si incorporation and higher bias voltage were increased.
(3) From the typical SEM images, the pitting corrosion of DLC films as an increase of bias voltage and addition of Si element was not as severe as those of other coatings.

Acknowledgements

The authors are grateful for the support provided by the Korea Science and Engineering Foundation (KOSEF) for the Korea-Canada Joint Research Project.

References

[1] Karim Bordji, Jean-Yves Jouzeau, Didier Mainard, Elisabeth Payan, Jean-Pierre Delagoutte, Patrick Netter, Biomaterials 17 (1996) 491.
[2] M. Donachie, Biomed. Alloys 7 (1998) 63.
[3] H. Kim, J.J. Lee, J. Kor. Inst. Met. Mater. 16 (2003) 11.
[4] A.C. Evans, J. Franks, P.J. Revell, Med. Device Technol. 5 (1991) 26.
[5] R. Lappalained, H. Heinomen, A. Anttila, S. Santavirta, Diamond Relat. Mater. 7 (1998) 482.

[6] X.-Z. Ding, F.-M. Zhang, X.-H. Liu, P.W. Wang, W.G. Durrer, W.Y. Cheung, S.P. Wong, I.H. Wilson, Thin Solid Films 246 (1999) 82.
[7] K. Enke, H. Dimigen, H. Hübsch, Appl. Phys. Lett. 36 (1980) 291.
[8] E.H.A. Dekempeneer, R. Jacobs, J. Smeets, J. Meneve, L. Eersels, B. Blanpain, J.R. Roos, D.J. Oostra, Thin Solid Films 217 (1992) 56.
[9] V.V. Sleptsov, V.M. Elinson, N.V. Simakina, A.N. Laymin, I.V. Tsygankov, A.A. kivaev, A.D. Musina, Diamond Relat. Mater. 5 (1996) 483.
[10] L. Tang, C. Tsai, W.W. Gerberich, L. Kruckeberg, D.R. Kania, Biomaterials 16 (1995) 483.
[11] D.P. Dowling, P.V. Kola, K. Donnellly, T.C. Kelly, K. Brumitt, L. Lloyd, R. Eloy, M. Therin, N. Weill, Diamond Relat. Mater. 6 (1997) 390.
[12] L. Chandra, M. Allen, R. Butter, N. Rushton, A.H. Lettington, T.W. Clyne, Diamond Relat. Mater. 4 (1995) 852.
[13] R. Butter, M. Allen, L. Chandra, A.H. Lettington, N. Rushton, Diamond Relat. Mater. 4 (1995) 857.
[14] F. Mansfeld, C.H. Tsai, Corrosion 49 (1993) 727.
[15] B. Matthes, E. Brozeit, J. Aromaa, H. Ronkainen, S.P. Hannula, A. Leyland, A. Matthews, Surf. Coat. Technol. 49 (1991) 489.
[16] Y.J. Yu, J.G. Kim, S.H. Cho, J.H. Boo, Surf. Coat. Technol. 162 (2003) 161.
[17] S. Rudenja, C. Leygraf, J. Pan, P. Kulu, E. Talimets, V. Miki, Surf. Coat. Technol. 114 (1999) 129.